

Status of proton detection efficiency  
measurement in E00102

Jeff Lachniet  
*Old Dominion University*  
*Department of Physics*

April 6, 2006

# 1 Introduction

A technique based on elastic ep scattering has been developed to measure the proton detection efficiency/trigger efficiency of the hadron (right) spectrometer in Hall-A for the E00102 experiment. The data set, analysis technique, and some results are described.

# 2 Data set selection

Runs from the so-called “qq” kinematic setting, which corresponds to parallel kinematics were chosen. For all runs in E00102, the electron (left) spectrometer angle was set to 12.5 degrees, and was never moved. The hadron arm was moved to the left and right of the momentum transfer vector in a pairwise fashion to  $\pm\phi_h$ . As the arm was swung past the  $\vec{q}$  direction, runs were taken in parallel kinematics. The runs used for this analysis, along with the prescale factors for different trigger types, are shown in Table 1.

Run number	PS3	PS5
2082	2440	1
2084	1500	1
2086	1500	1
2088	1500	1
2090	1500	1
2803	200	1

Table 1: Runs used for this analysis.

The PS entries in the tables refer to the prescale factors for the two trigger type used for this analysis, T3 and T5. The T3 trigger is a single-arm electron trigger, and the T5 trigger is an electron-proton two arm coincidence trigger.

These runs listed in Table 1 were all taken with the 0.868652 msr collimator in place. Other qq kinematics runs exist, but several of them were taken using the sieve-slit collimator. This is great for optics calibrations, but complicates this analysis, so sieve-slit runs were excluded. A few other runs were taken with the 0.365918 msr collimator in place. These runs were also excluded.

The data used were from the July 2004 replay (located on the silo at /mss/halla/e00102/replay\_Jul2004). The July 2004 replay was done using ESPACE. The ESPACE hbook files were converted to ROOT TTree objects using the h2root utility.

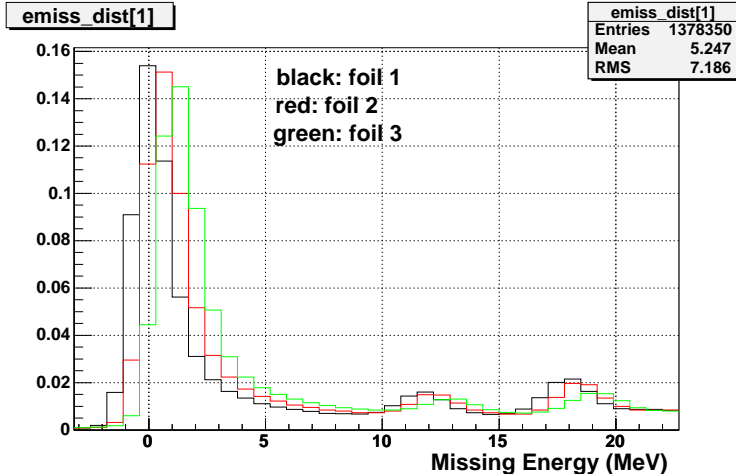


Figure 1: Normalized missing energy distributions in ep coincidence events for the three water foils. Black: foil 1, Red: foil 2, Green: foil 3

### 3 Method

The method used to analyze the proton detection efficiency is based on elastic ep scattering from the hydrogen nuclei in the waterfall target. Elastic ep coincidence events are counted, as are single arm elastic electron events where no proton was seen in the hadron arm. The proton detection efficiency can then be determined from:

$$\eta_p = \frac{N_C}{N_C + N_A} \tag{1}$$

where  $N_C$  is the number of ep coincidences, and  $N_A$  is the number of anti-coincidence events where elastic electron is seen, but no proton is seen.

## 4 Elastic electron-proton coincidence selection

### 4.1 Missing energy cuts

Elastic coincidence events are selected using a cut on the missing energy. The missing energy distribution for coincidence events in each of three water-foils is shown in Fig 1.

Notice that the missing energy distributions for the three foils are shifted relative to each other. This suggests that the energy loss corrections in ES-PACE were not handled correctly. Inelastic events were excluded by requiring  $E_{missing} < E_{max}$ . The  $E_{missing}$  cutoff values for the three foils are listed in Table 2.

foil	$E_{max}$ (MeV)
1	5.0
2	5.6
3	6.2

Table 2: Missing energy cuts for elastic coincidence event selection.

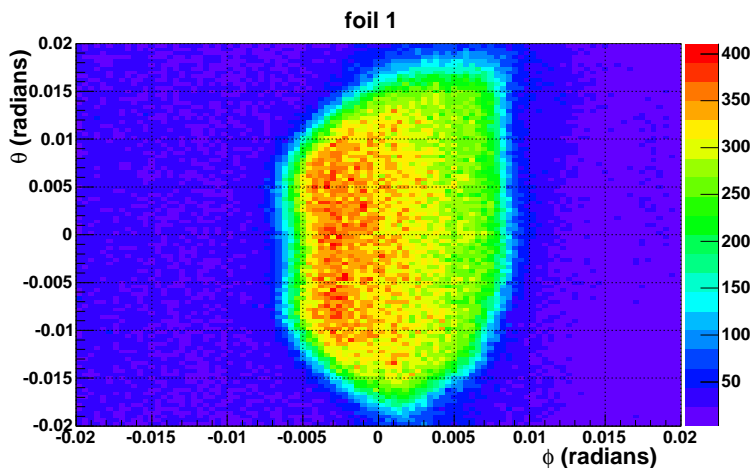


Figure 2: Angular distribution of electrons in ep coincidence events in foil 1.

The choice of cut for foil 1 was somewhat arbitrary. The cuts for the other two were determined by shifting the foil 1 cut by an amount equal to the shift in the peak location in the  $E_{missing}$  distribution for that foil relative to foil 1.

## 4.2 Angular cuts

The distribution of electrons in the  $(\phi, \theta)$  plane for the three foils are shown in Figs. 2,3,4. Recall that  $\phi$  is the in-plane scattering angle, measured relative to  $\phi_0 = 12.5^\circ = 0.21817rad$  and  $\theta$  is the out-of-plane scattering angle, measured relative to  $\theta_0 = 0$ .

A set of  $\theta$  cuts were chosen to remove the “triangular” regions at the top and bottom of the  $(\phi, \theta)$  distributions. The cuts used are listed in Table 3.

foil	$\theta_{min}(rad)$	$\theta_{max}(rad)$
1	-0.007	0.006
2	-0.01	0.009
3	-0.01	0.01

Table 3: Allowed  $\theta$  range for elastic electrons.

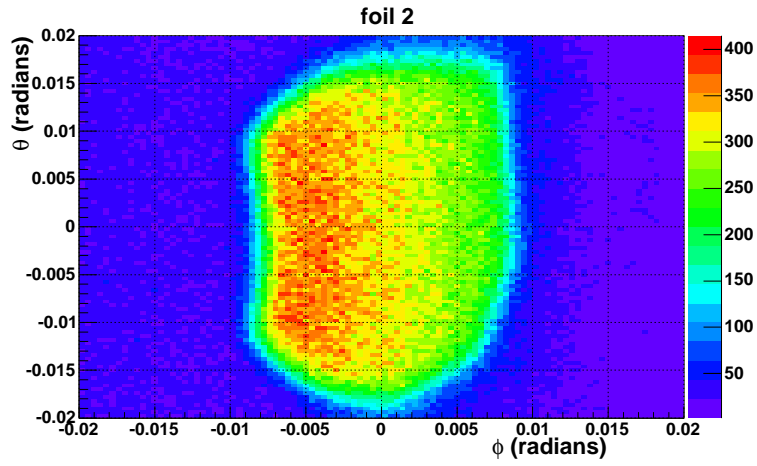


Figure 3: Angular distribution of electrons in ep coincidence events in foil 2.

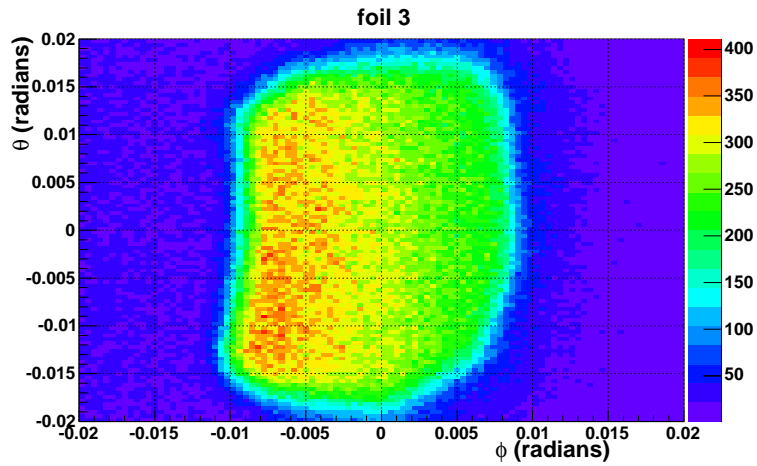


Figure 4: Angular distribution of electrons in ep coincidence events in foil 3.

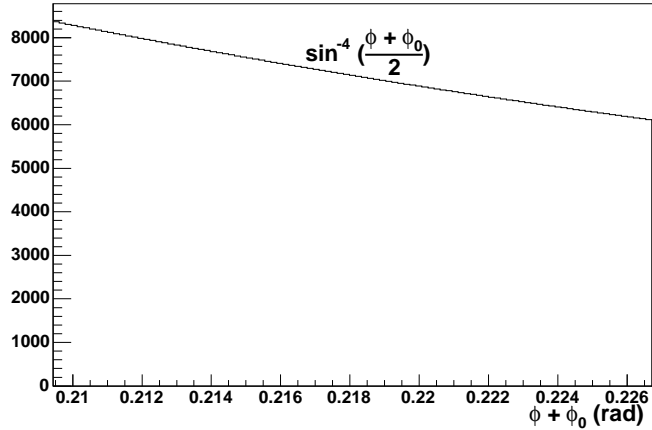


Figure 5: Angular dependence of Mott cross-section.

The choice of these cuts is somewhat arbitrary, but the measured efficiency is seen to be fairly insensitive to small variation in the values used.

The ep cross-section has no functional dependence on the out-of-plane angle  $\theta$ , but this is not the case for the in-plane angle  $\phi$ . The ep cross-section contains a factor of the Mott cross-section, which varies like  $\sin^{-4}(\frac{\phi+\phi_0}{2})$ . A plot of this quantity is shown in Fig. 5. The  $\phi+\phi_0$  distributions of coincidence events satisfying  $-0.005 < \theta < 0.005$  originating in each of the three water-foils are shown in Fig 6,7 and 8. Recall that  $\phi_0$  is 0.2182 radians

The  $\phi$  cut for each foil was chosen to keep the smoothly varying slanted-line portion of the distribution which resembled Fig 5 and throw out the portion at the edges where the acceptance is rapidly changing. The  $\phi$  cuts used are summarized in Table 4

foil	$\phi_{min}(rad)$	$\phi_{max}(rad)$
1	-0.004	0.006
2	-0.005	0.006
3	-0.006	0.006

Table 4: Allowed  $\phi$  range for elastic electrons.

### 4.3 $\Delta E$ distribution

After applying the  $E_{miss}$  and  $(\phi, \theta)$  cuts, the quantity:

$$\Delta E = E_{measured} - E_{elastic}(\Theta_s) \quad (2)$$

was calculated. Here,  $E_{measured}$  is the electron energy measured by the spectrometer, and  $E_{elastic}(\Theta_s)$  is the energy expected for an electron elastically

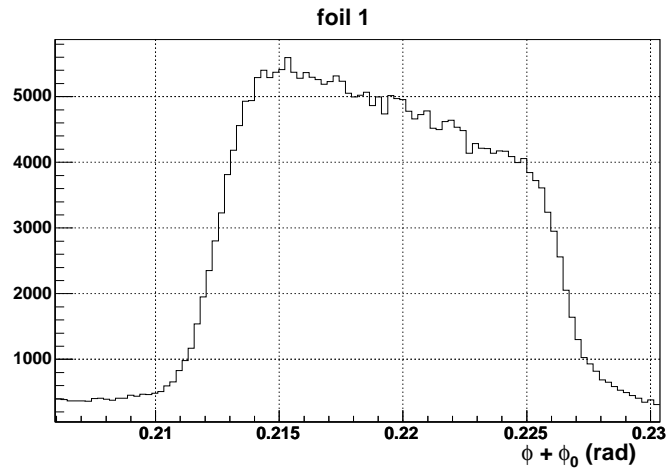


Figure 6:  $\phi + \phi_0$  distribution for coincidence events originating in foil 1 and satisfying  $-0.005 < \theta < 0.005$ .

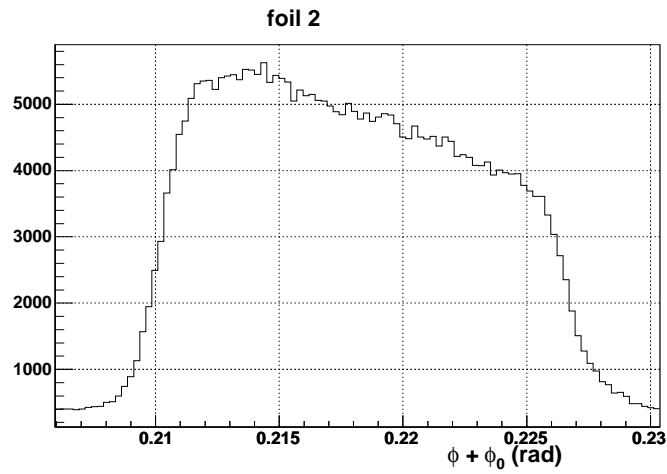


Figure 7:  $\phi + \phi_0$  distribution for coincidence events originating in foil 2 and satisfying  $-0.005 < \theta < 0.005$ .

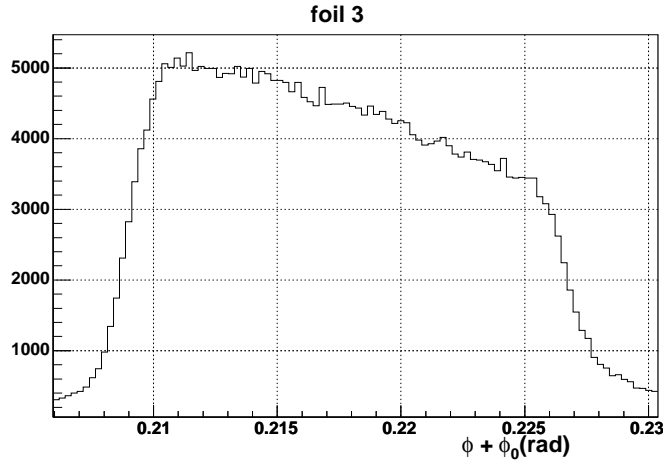


Figure 8:  $\phi + \phi_0$  distribution for coincidence events originating in foil 3 and satisfying  $-0.005 < \theta < 0.005$ .

scattered through an angle  $\Theta_s$ . Note that  $\Theta_s$  is not the in-plane angle  $\phi$  or the out-of-plane angle  $\theta$ , but the angle between the incident electron momentum and the scattered electron momentum. These angles are related by:

$$\cos \Theta_s = \frac{\cos \phi_0 + \tan \phi \sin \phi_0}{\sqrt{1 + \tan^2 \phi + \tan^2 \theta}}. \quad (3)$$

The energy expected for an electron elastically scattered through an angle  $\Theta_s$  is:

$$E_{elastic}(\Theta_s) = \frac{E_0}{1 + \frac{E_0}{M_p}(1 - \cos \Theta_s)} \quad (4)$$

The  $\Delta E$  distributions for accepted coincidence events originating in each of the three foils are shown in Fig 9.

## 5 Elastic anti-coincidence spectrum

Next the data set was scanned for anti-coincidence elastic ep events, events where an elastically scattered electron is seen in the left-arm, and **no** event is seen in the right-arm. These events are collected by the T3 trigger type. The T3 prescale factors for the runs used in this analysis are shown in Table 1

### 5.1 Fiducial cut

T3 events are selected in which the detected electron satisfies the same cuts in the  $(\phi, \theta)$  plane that were imposed on electrons in the coincident events. The cuts are listed in Tables 3, 4.

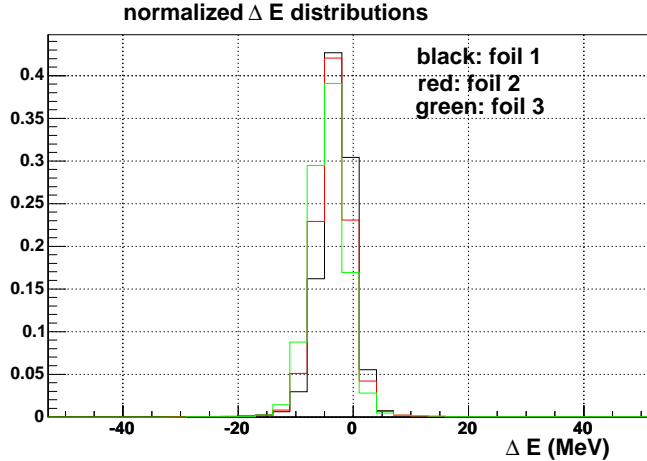


Figure 9: Normalized  $\Delta E$  distributions for accepted ep coincidence events originating in each of the three water-foils. Black: foil 1, Red: foil 2, Green: foil 3.

## 5.2 $\Delta E$ distribution

The quantity  $\Delta E$  was calculated for each T3 event which passed the angular cuts. The distribution of  $\Delta E$ , summed over all events from all three foils, is shown in Fig 10. Notice that unlike the coincidence event spectrum, where we could use an missing energy cut to remove inelastic events, there is significant inelastic background.

Histograms of the type shown in Fig 10 were also generated for each foil separately. In producing these histograms, the entries were **not** weighted by the T3 prescale factors for the run.

## 5.3 Background subtraction

An attempt was made to remove the inelastic background from the anti-coincidence  $\Delta E$  spectrum. The error bars (statistical only,  $\sqrt{N}$  in each bin) on the  $\Delta E$  histogram in the region where the elastic peak was seen in the coincidence spectrum,  $-20\text{MeV} < \Delta E < 15\text{MeV}$ , were set to a large number. This was a lame hack whose effect was to exclude these points from the fit. After adjusting the errors, a fourth order polynomial was fit to the  $\Delta E$  spectrum over the range  $-50\text{MeV} < \Delta E < 50\text{MeV}$ . The fit, for the all-foils histogram is shown in Fig 11.

Fits of the type shown in Fig 11 were also generated for each foil separately. The value of the polynomial at the center of each bin was subtracted from the bin contents to produce the background subtracted  $\Delta E$  distribution shown in Fig 12.

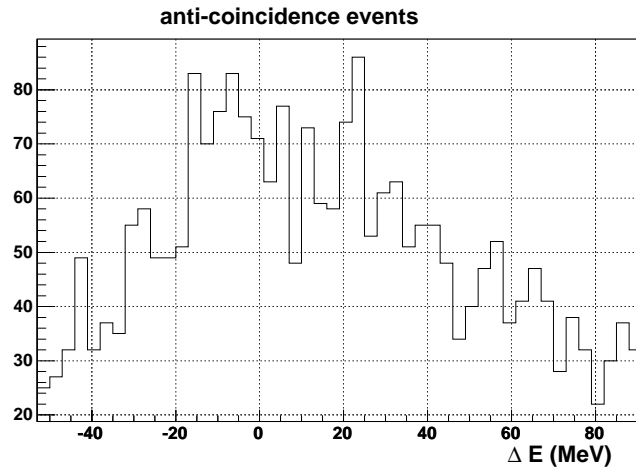


Figure 10:  $\Delta E$  distribution for anti-coincidence events from all three foils.

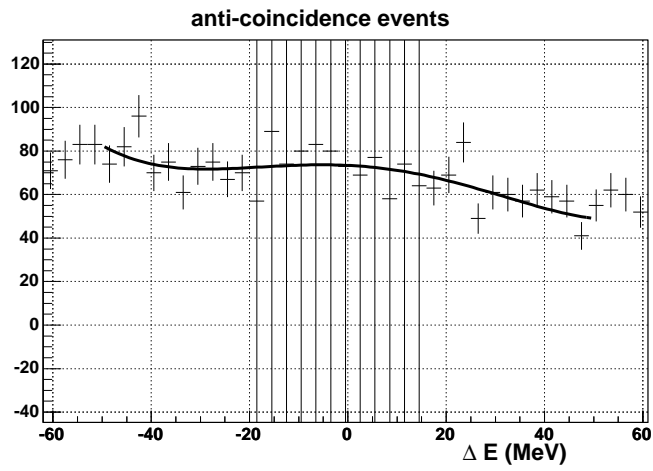


Figure 11:  $\Delta E$  distribution for anti-coincidence events from all three foils and polynomial fit to background.

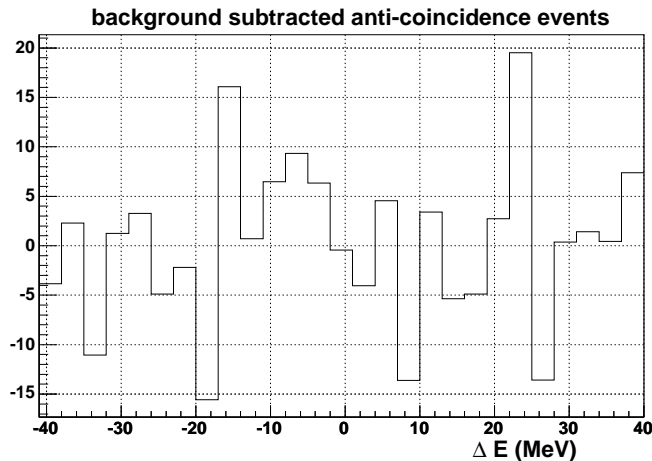


Figure 12: Background subtracted  $\Delta E$  distribution for anti-coincidence events from all three foils.

#### 5.4 Efficiency determination

The coincident and unsubtracted anti-coincident  $\Delta E$  spectra were both integrated over the range  $-20 < \Delta E < 15 \text{ MeV}$ . This range was chosen by visual inspection of the coincident spectrum. The background fit was also integrated over this range. Note that the prescale factor for coincident events (T5 triggers) was set to 1 for all runs, but the electron single-arm event (T3 triggers) prescale factor varied from run to run. In producing the anti-coincident spectrum, events were filled into the histogram with unit weighting, **not** weighting by the prescale factor for the run the event was taken from. An “effective prescale factor” was calculated for T3 triggers:

$$PS_{eff} = \frac{1}{N} \sum_{i=0}^N PS_i \quad (5)$$

where  $N$  is the total number of anti-coincident events observed, and  $PS_i$  is the run dependent prescale factor for the  $i^{th}$  event. The proton efficiency is then calculated from:

$$\eta_p = \frac{N_C}{N_C + PS_{eff}M} \quad (6)$$

where  $N_C$  is the integrated number of events under the elastic peak in the coincidence histogram, and  $M = N_A - N_B$  is the difference between the integrated number of events in the elastic peak in the unsubtracted anti-coincidence spectrum ( $N_A$ ) and the integrated number of events in the elastic peak region of the background fit ( $N_B$ ).

## 5.5 Uncertainty estimate

An attempt to quantify the statistical uncertainty in this procedure was made. The efficiency can be rewritten as:

$$\eta = \frac{1}{1 + PS\alpha} \quad (7)$$

where  $PS$  is the effective prescale factor and  $\alpha = \frac{M}{N_C}$ . The standard propagation of errors formula was applied:

$$\sigma_\eta^2 = \sigma_\alpha^2 \left( \frac{\partial \eta}{\partial \alpha} \right)^2 \quad (8)$$

Taking derivatives,

$$\frac{\partial \eta}{\partial \alpha} = \frac{-PS}{(1 + PS\alpha)^2} \quad (9)$$

$$= -\eta^2 PS. \quad (10)$$

Again applying the standard propagation of errors formula,

$$\left( \frac{\sigma_\alpha}{\alpha} \right)^2 = \left( \frac{\sigma_M}{M} \right)^2 + \left( \frac{\sigma_{N_C}}{N_C} \right)^2 \quad (11)$$

We take  $\sigma_{N_C} = \sqrt{N_C}$ , so that

$$\frac{\sigma_{N_C}}{N_C} = \frac{1}{\sqrt{N_C}} \quad (12)$$

For the other term in Eqn 11, we have  $M = N_A - N_B$ . If we neglect the error in the fit and take  $\sigma_{N_A} = \sqrt{N_A}$ , then we have:

$$\frac{\sigma_M}{M} = \frac{\sqrt{N_A}}{N_A - N_B} \quad (13)$$

Putting all of these pieces together, we get:

$$\sigma_\eta = \alpha \eta^2 PS \sqrt{\frac{N_A}{(N_A - N_B)^2} + \frac{1}{N_C}} \quad (14)$$

## 6 Results

The proton efficiency was measured separately for each water-foil, and also for the full target. The results obtained using the efficiency and error formulas described above are summarized in Table 5.

Foil	$N_C$	$N_A$	$N_B$	$PS_{eff}$	efficiency	uncertainty
all	681183	878	870.109	842.213	0.990338	0.0359312
1	169674	203	194.834	827.823	0.961686	0.0642892
2	254849	331	326.949	854.474	0.986601	0.0593763
3	256660	344	339.55	838.592	0.98567	0.0588756

Table 5: Proton efficiency results

The results seem to be stable against small variations in the choice of the angular cuts. The efficiency results show more sensitivity to variation in the integration range used for the  $\Delta E$  peak. For example, if the region of integration is narrowed to  $-15\text{MeV} < \Delta E < 10\text{MeV}$ , the efficiencies change to the values shown in Table 6. The observed changes in efficiency are probably due to unreliability of the background fitting and subtraction procedure (the low statistics aren't helpful), although the two results agree within the statistical uncertainties. No attempt has been made (yet) to quantify any systematic error associated with this measurement.

Foil	$N_C$	$N_A$	$N_B$	$PS_{eff}$	efficiency	uncertainty
all	680114	757	727.072	842.213	0.964263	0.0316796
1	169439	171	165.16	827.823	0.972259	0.060393
2	254386	282	272.853	854.474	0.970192	0.0530941
3	256289	304	280.355	838.592	0.928189	0.049151

Table 6: Proton efficiency results, using a more narrow  $\Delta E$  region.